J Mol Evol (2000) 51:464–470
DOI: 10.1007/s002390010109

JOURNAL OF MOLECULAR EVOLUTION

Nonenzymatic Oligomerization on Templates Containing Phosphodiester-Linked Acyclic Glycerol Nucleic Acid Analogues

John C. Chaput, Christopher Switzer

Department of Chemistry, University of California, Riverside, CA 92521, USA

Received: 2 May 2000 / Accepted: 1 August 2000

Abstract. Nonenzymatic oligomerization reactions represent a model for studying the prebiotic replication of informational macromolecules. To explore the fitness of acyclic oligonucleotides in these reactions, we have synthesized a series of DNA hairpins appended with templates incorporating atactic glyceryl cytosine residues. Atactic glyceryl cytosine units are found to impede, but not to block, template-directed oligomerization of guanosine 5′-phosphoro-2-methylimidazole (2-MeImpG). Evidence suggests that both D and L glyceryl nucleoside configurations at a given template position contribute to product formation. The stability of DNA duplexes bearing isolated glyceryl cytosine residues has also been investigated. Duplex thermal denaturation experiments indicate that an atactic glyC · dG base-pair is intermediate in stability between a dC · dG pair and a dT · dG mismatch.

Key words: Template-directed oligomerization — Chemical evolution — Pre-RNA

Introduction

The search for an ancestral informational biopolymer capable of both replication and catalysis is a formidable challenge. Within this context, RNA has been the most thoroughly explored among extant biopolymers (Orgel 1992; Joyce 1987). Although discoveries of increasingly diverse RNA catalysts (Unrau and Bartel 1998; Frauendorf and Jaschke 1998; Tarasow et al. 1997; Joyce 1996) enhance the attractiveness of RNA as a precursor to protein enzymes in molecular evolution, it remains difficult to conceive of a direct transition from prebiotic reagents to an RNA world. The need to synthesize prebiotically significant quantities of replication competent monoribonucleotides that contain four stereogenic carbon atoms based on a sugar that is unstable under conditions possibly prevalent on the primitive Earth is one of many obstacles (Larralde et al. 1995; Joyce 1989). Effects of chirality are underscored by template copying experiments conducted with only 2 of the 16 possible stereoisomers of a single activated RNA monomer, D-GMP and L-GMP, that show that the L-isomer effectively inhibits oligomerization of the D-isomer on a D-polynucleotide template (Joyce et al. 1984a). As an alternative, RNA may have been preceded in evolution by a simpler nucleic acid-like structure capable of catalysis and information storage, pre-RNA. A polymer system in which hydroxymethyl glycerol bearing a single stereogenic carbon center replaces ribose has been proposed as one alternative (Spach 1984; Joyce et al. 1987). Models suggest that glyceronucleotides may be less susceptible to enantiomer cross-inhibition owing to their backbone flexibility (Joyce et al. 1987; Merle et al. 1995).

Tests of glyceronucleotides to date focusing on the thermodynamics of helix formation between glycero- and deoxyribonucleotide strands have met with mixed results (Schneider and Benner 1990; Merle et al. 1995). For example, while Benner has shown that isotactic $glyT_{12} \cdot dA_{12}$ does not associate (Schneider and Benner 1990), Merle et al. (1995) have observed that atactic

Correspondence to: Christopher Switzer; e-mail: switzer@citrus.ucr.edu

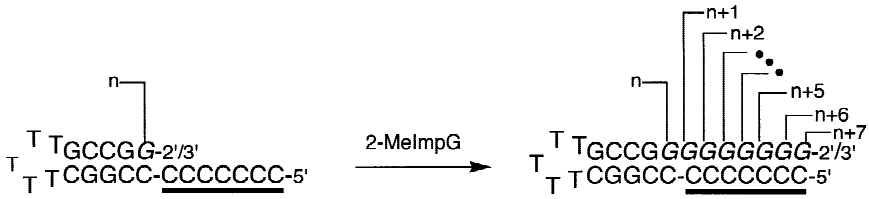

Fig. 1. Template-directed oligomerization on a glyceryl cytosine alternative nucleic acid template grafted to a natural DNA hairpin.

$glyA_{12} \cdot dT_{12}$ forms a stable complex. It is ultimately unclear, however, how strongly correlated duplex stability and template-directed oligomerization reaction kinetics might be in these systems. Herein we probe the nonenzymatic oligomerization of guanosine 5′-phosphoro-2-methylimidazolide (2-MeImpG) on DNA hairpin templates containing atactic glyceryl cytosine (glyC) residues (Fig. 1) to assess further the potential for replication with acyclic nucleotides.

Materials and Methods

General Methods

Proton (^{1}H) NMR and phosphorus (^{31}P) NMR spectra were recorded on a Varian Inova-300 (300 and 125 MHz, respectively) spectrometer. Mass spectra (MS) and exact mass spectra were recorded on a VG-ZAB-2FHF spectrometer using FAB ionization by the staff of the Southern California Regional Mass Spectrometry Facility (University of California, Riverside). Ultraviolet spectra were obtained with a Hewlett–Packard 8452A diode array spectrophotometer. All experiments involving air and/or moisture sensitive materials were carried out under an argon (Ar) atmosphere. Reagents were purchased from Sigma, Aldrich, and Fluka chemical companies. Solvents were purchased from Fisher Scientific. T4 polynucleotide kinase and ribonuclease T1 were purchased from Boehringer Mannheim. 5′-[γ-^{32}P]ATP (~3000 Ci/mmol) was purchased from Amersham. DNA synthesis reagents, phosphoramidites, and controlled pore glass support were purchased from Glen Research. Pyridine and CH_2Cl_2 were freshly distilled over CaH_2 as needed. The synthesis of guanosine 5′-phosphoro-2-methylimidazolide (Joyce et al. 1984b) and (1′,3′-dihydroxy-2′-propoxy)methyl cytosine, **1** (Ogilvie et al. 1983), was performed as described previously.

GlyC Monomer Synthesis

4-N-*Benzoyl-[(1′,3′-Dihydroxy-2′-Propoxy)Methyl]Cytosine **(2).*** To a solution of glycerol nucleoside, **1** (430 mg, 2.0 mmol), in 20 ml pyridine at 0°C was added trimethylsilyl chloride (1.3 ml, 10 mmol), and after 30 min benzoyl chloride (1.2 ml, 10 mmol) was added. The reaction mixture was brought to room temperature (RT) and left stirring for 3 h, then cooled to 0°C and quenched with cold H_2O (2 ml) and 28% NH_4OH (2 ml) following a 15-min wait between additions. The resulting mixture was concentrated under reduced pressure, dissolved in CH_2Cl_2 (50 ml), washed with 10% HCl (3 × 10 ml), dried over $MgSO_4$, filtered, and concentrated under reduced pressure. The crude residue was purified by flash chromatography (SiO_2, 5–10% MeOH/CH_2Cl_2) to afford **2** (441 mg) in a 69% yield. ^{1}H NMR (DMSO): δ 3.35–3.4 (m, 4H), 3.59 (m, 1H), 4.65 (t, 2H), 5.34 (s, 2H), 7.31 (d, 1H, J = 6.75 Hz), 7.52 (t, 2H, J = 7.74, 7.33 Hz), 7.63 (t, 1H, J = 7.33, 7.29 Hz), 8.01 (d, 2H, J = 7.43 Hz), 8.20 (d, 1H, J = 6.94 Hz), 11.21 (s, 1H). MS (EI^+): *m/z* 319. Exact mass (EI^+): calcd for $C_{15}H_{17}N_3O_5$ (MH^-), 319.116821; found, 319.1159.

4-N-*Benzoyl-[(1′*-O-*(4,4′-Dimethoxytrityl)-2′-Propoxy)Methyl]-Cytosine **(3).*** To a solution of nucleoside, **2** (435 mg, 1.4 mmol), in 5 ml pyridine at 0°C was added dimethoxytrityl chloride (475 mg, 1.4 mmol). After stirring for 3 h at RT, CH_2Cl_2 (50 ml) was added and the reaction mixture was washed with $NaHCO_3$ (3 × 10 ml), dried over Na_2SO_4, filtered, and concentrated under reduced pressure. The crude residue was purified by flash chromatography (SiO_2, 2–5% MeOH/CH_2Cl_2) to afford **3** (238 mg) in a 30% yield. ^{1}H NMR ($CDCl_3$): δ 2.63 (s, 1H), 3.22 (d, 2H), 3.65 (m, 2H), 3.78 (s, 6H), 3.90 (m, 1H), 5.42 (q, 2H), 6.81 (d, 4H), 7.20–7.31 (m, 8H), 7.4 (d, 2H, J = 7.48 Hz), 7.51 (t, 2H, J = 7.68, 7.31 Hz), 7.61 (d, 1H, J = 7.26 Hz), 7.68 (t, 1H, J = 7.57, 7.85 Hz), 7.80 (d, 1H, J = 7.15 Hz) 7.91 (d, 2H, J = 7.30 Hz), 8.61 (s, 1H). MS (FAB^-): *m/z* 620. HRMS (FAB^-): calcd for $C_{36}H_{35}N_3O_7$ (MH^-), 620.239676; found, 620.2378.

4-N-*Benzoyl-1-[1′*-O-*(4,4′-Dimethoxytrityl)-2′-propoxy)Methyl]-Cytosine 2-Cyanoethyl* N,N′*-Diisopropylphosphoramidite **(4).*** To a solution of nucleoside, **3** (235 mg, 0.38 mmol), and diisopropyl ammonium tetrazolide (34 mg) in 5 ml acetonitrile was added diisopropylamino cyanoethyl phosphordiamidite (0.13 ml, 0.4 mmol). After stirring for 5 h at RT, CH_2Cl_2 (20 ml) was added and the reaction mixture was washed with $NaHCO_3$ (1 × 10 ml), dried over Na_2SO_4, filtered, and concentrated under reduced pressure. The crude residue was purified by flash chromatography (SiO_2, 50% EtOAc/1% pyridine/hexane) to afford **4** (128 mg) in a 40% yield. ^{1}H NMR ($CDCl_3$): δ 1.08–1.18 (m, 12H), 2.6 (m, 2H), 3.22 (m, 2H), 3.52 (m, 2H), 3.61–3.74 (m, 4H), 3.77 (s, 6H), 4.01 (m, 1H), 5.45 (q, 2H), 6.82 (m, 4H), 7.16–7.31 (m, 9H), 7.41 (d, 2H), 7.5 (t, 2H), 7.6 (t, 1H), 7.92 (t, 1H). ^{31}P NMR ($CDCl_3$): δ 148.52, 148.34. MS (FAB^+): *m/z* 844. HRMS (FAB^+): calcd for $C_{45}H_{52}N_5O_8PNa$ (MNa^+), 844.345122; found, 844.3482.

DNA Synthesis. Solid-phase oligodeoxynucleotide synthesis was performed on an ABI 391EP synthesizer (Applied Biosystems) using commercially available reagents and phosphoramidites. The modified cytosine phosphoramidite, chemically synthesized as described above, was incorporated into oligonucleotides with efficiencies comparable to the commercially available natural phosphoramidites. All oligonucleotides were synthesized trityl-off (1-μmol scale) on a CPG solid support derivatized with a riboguanosine nucleoside bearing a 3′-*O*-acetyl protecting group (Glen Research). Cleavage from the solid support and deprotection was accomplished in concentrated NH_4OH for 16 h at 55°C. Oligonucleotides were purified by preparative gel electrophoresis and quantified by UV absorbance at 260 nm and 70°C. The extinction coefficients for the natural nucleotides used for the calculation were as follows: dCMP, 7050; TMP, 8840; dGMP, 12,010; and C′MP, taken as CMP.

5′-Radiolabeling Procedure

Oligonucleotide (100 pmol) was combined with 6 μl H_2O, 1 μl 10× kinase buffer (700 m*M* Tris–HCl, pH 7.6, 100 m*M* $MgCl_2$, 50 m*M*

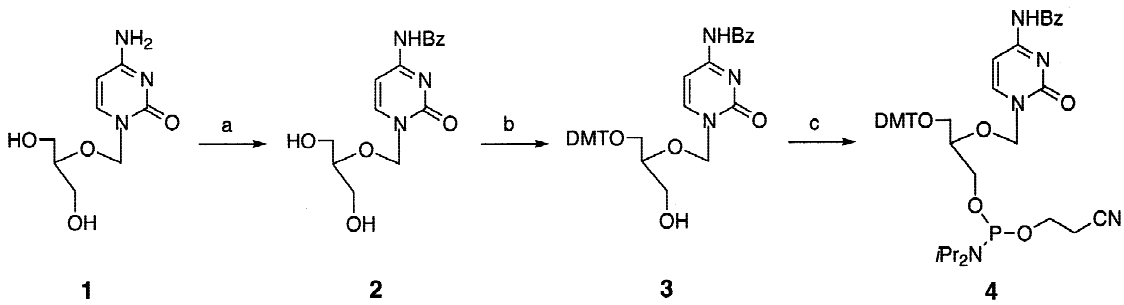

Fig. 2. Synthesis of the glyceryl cytosine phosphoramidite **4: (a)** TMSCl, BzCl, NH_4OH (69%); **(b)** DMTCl/pyridine (30%); **(c)** diisopropyl ammonium tetraazolide/bis-diisopropylamino cyanoethyl phosphordiamidite (40%).

DTT), 1 μl [γ-^{32}P]ATP (2 μCi; Amersham), and 1 μl T4 polynucleotide kinase (3 U; Amersham). The samples were incubated for 30 min at 37°C, after which time 1 μl ATP (660 μ*M*) was added, followed by incubation for an additional 30 min at 37°C. Radiolabeled oligonucleotides were desalted on a NAP-25 column (Pharmacia) and concentrated to dryness.

Oligomerization Reaction Conditions

Template reactions were carried out in Eppendorf tubes in a total volume of 20 μl using the general procedure described by Wu and Orgel (1992). 5′-^{32}P-Labeled-oligonucleotide (10 pmol), 10 μl NaCl (2 *M*), and 4 μl $MgCl_2$ (1 *M*) were combined and concentrated to dryness. The residue was dissolved in 8 μl 2,6-lutidine–HCl buffer (0.5 *M*, pH 8.0), and 9 μl H_2O. Samples were then heated for 5 min at 55°C and cooled for 5 min at RT and then 5 min at 0°C. The reaction was initiated by the addition of a freshly prepared solution of 2-MeImpG (3 μl; 21.3 OD/rxn; final concentration, ~100 m*M*). After 10 days at 5°C, 10 μl of a 7 *M* urea/1× TBE/0.1% bromophenol blue/0.1% xylene cyanol solution was added and 15 μl of the resulting mixture was subjected to 20% denaturing PAGE analysis.

Ribonuclease T1 Digestion

Gel-purified oligomerization product (~1 pmol) was dissolved in 9 μl Tris–EDTA buffer (10 m*M* Tris–HCl, pH 7.4, 1 m*M* EDTA, pH 8.0) along with 1 μl $tRNA^{Phe}$ (10 mg/ml). The reaction was heated for 10 min at 55°C then centrifuged, 1 μl ribonuclease T1 (100 U; Boehringer Mannheim) was added, and heating was continued at 55°C for the times indicated in the figure legends. The reaction mixture was quenched with 5 μl of a 7 *M* urea/1× TBE/0.1% bromophenol blue/0.1% xylene cyanol solution and subjected to 20% denaturing PAGE analysis. Bands were quantitated using a phosphorimager and ImageQuant software (Molecular Dynamics).

Melting Experiments

UV absorbance-versus-temperature profiles were measured on a Varian Cary 500 spectrophotometer in a temperature-controlled cell holder with a Varian peltier temperature controller. The absorbance was recorded in the reverse and forward directions at temperatures of 25 to 90°C at a rate of 1°/min. Experiments were performed in duplicate with different samples and T_m's were averaged. All melts were done in 1 *M* NaCl, 10 m*M* Na_2HPO_4, pH 7, 0.1 mM EDTA, pH 7, and a 5 μ*M* total oligonucleotide concentration. Duplex free energy values were determined from melting curves by nonlinear regression curve-fitting using a two-state model according to the method of Turner (Longfellow et al. 1990).

Results and Discussion

Chemical Synthesis and Design of Atactic Glycerol Templates

Acyclic nucleoside **1** was synthesized as reported (Ogilvie et al. 1983) and then converted to phosphoramidite **4** in analogy with the synthesis of standard phosphoramidites (Fig. 2). This transformation involved protection of the exocyclic amino group of **1** as a benzoyl derivative, subsequent introduction of a dimethoxytrityl hydroxyl protecting group, and phosphitylation to afford glycerol phosphoramidite **4**, in a modest yield. Solid-phase synthesis of DNA hairpin templates **6–9** incorporating glyceryl cytosine at the positions indicated (Fig. 3) was performed beginning on a *ribo*G derivatized CPG column. Hairpin templates were obtained in a high yield and purified by preparative gel electrophoresis. These templates are modeled after those first reported by Wu and Orgel (1992). Previously, our laboratory has employed this system to demonstrate mononucleotide oligomerization on templates bearing 2′,5′-linked RNA (Prakash et al. 1997).

Nonenzymatic Oligomerization on (Partially) Atactic Templates

Oligomerization reactions on ^{32}P-end-labeled templates **5–9** were performed by incubation with 2-MeImpG (Inoue and Orgel 1981) in the presence of $MgCl_2$ for 10 days. The extent of oligomerization was assayed by electrophoresis on denaturing 20% polyacrylamide gels and visualization by autoradiography and phosphorimaging. An autoradiogram of a representative oligomerization experiment is shown in Fig. 4.

Oligomerization on the dC_7 template **5** in lane 1 in Fig. 4 was performed as a control for template-directed reactions on glyC-containing templates in the other lanes. As reported previously, a dC_5 hairpin template will direct the synthesis of full-length product after approximately 7 days (Wu and Orgel 1992). Comparison of the glyC-bearing templates in lanes 2–5 to the control dC_7 template in lane 1 indicates some degree of full-length

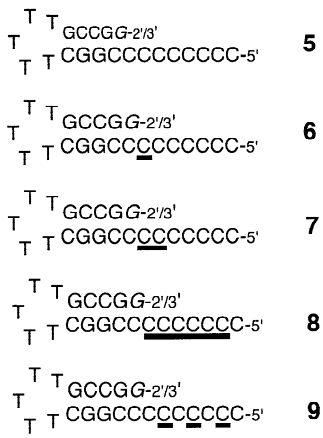

Fig. 3. Hairpin templates used in oligomerization reactions. Underlined regions refer to glyceryl cytosine residues. Terminal 3′-riboG residues are *italicized.* DNA regions are in standard type.

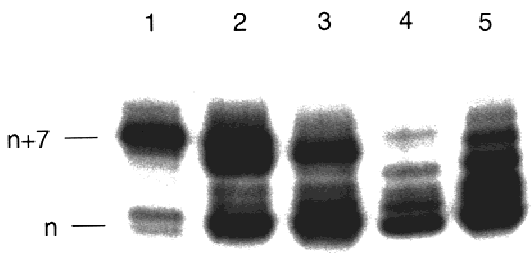

Fig. 4. Autoradiogram after 20% PAGE analysis of 2-MeImpG oligomerization on templates **5–9** after 10 days. Lanes 1–5 correspond to templates **5–9,** respectively.

product formation for each of the four glyC-bearing templates investigated, although the efficiencies of product formation vary widely.

Oligomerizations on $glyCdC_6$ and $glyC_2dC_5$ in lanes 2 and 3 in Fig. 4 demonstrate that single or consecutive glyC residues are impediments to primer extension. In these two cases and the case of dC_7 it proved possible to quantitate the amount of unreacted template by phosphorimager analysis. Thus in the $glyCdC_6$ and $glyC_2dC_5$ reactions there was found to be 25 and 60%, respectively, unreacted hairpin template after 10 days. This may be compared to the dC_7 reaction, where approximately 3% unreacted template was observed under the same conditions. Templates $glyC_6dC$ and $(dCglyC)_3dC$ in lanes 4 and 5 were found to be much less efficient at directing the incorporation of multiple G residues compared to templates $glyCdC_6$ and $glyC_2dC_5$. Although it was not possible to determine the amount of template remaining after 10 days for $glyC_6dC$ and $(dCglyC)_3dC$ due to the occurrence of nearby partially resolved bands, it was possible to estimate the relative quantity of the two slowest-moving electrophoretic bands in each of these reactions as ~5% compared to other products and unreacted template. The above data confirm the qualitative results apparent from Fig. 4, namely, that the relative efficiencies of the templates are dC_7 > $glyCdC_6$ > $glyC_2dC_5$ > $(dCglyC)_3dC \approx glyC_6dC$.

Effect of Template Chirality on Product Formation

Acyclic nucleotides have been proposed to be less susceptible to enantiomer cross-inhibition since both D and L forms are anticipated to adopt similar conformations (Joyce et al. 1987). Significantly, most informational polymers investigated to date have been subject to enantiomeric cross-inhibition. Template reactions of RNA, DNA, and PNA are all inhibited when incubated with racemic activated mononucleotide (Joyce et al. 1984a; Kozlov et al. 1999; Schmidt et al. 1997). Two exceptions are isotactic hexitol DNA templates, having been discovered to be enantioselective when challenged with a pool of racemic RNA monomer (Kozlov et al. 1999), and pyranosyl-RNA templates, which exhibit selectivity during ligative oligomerization (Bolli et al. 1997).

Template-directed reactions in the currently studied system examine the reversed situation of nonenzymatic oligomerization of enantiomerically pure monomers on stereochemically heterogeneous templates. Such a system models the chiroselectivity of glyceryl nucleotides in the context of a hypothetical transition from a pre-RNA entity to RNA, or "genetic takeover" (Cairns-Smith 1982). In this context it should be possible to assess if both the D and the L acyclic nucleotide isomers contained in the template are capable of directing the oligomerization of activated monomers based on the efficiency of their template-directed reactions.

Quantitation of the oligomerization products from $glyCdC_6$ suggests that both the "right" and the "wrong" acyclic cytidine diastereomeric templates may contribute to template-directed synthesis. This possibility derives from the formation of 75% n+1 or longer addition products from this template (lane 2, Fig. 4) and depends on at least two assumptions. The first is that no significant diastereoselection occurred during the purification of the template. Given that all templates were PAGE purified and only a single band was observed, it would seem unlikely that any diastereoselective enrichment would have occurred. The second assumption is that an alternative mechanism for template elongation that avoids the glyC residue not be operative. We note that if the single acyclic cytosine residue in the $glyCdC_6$ template were to assume an extrahelical conformation, then it might be possible for a residual helical dC_6 segment to template the formation of product. Template **7** ($glyC_2dC_5$) yields ~35% of n+6 and n+7 products and consequently also lends support to the contention that both diastereomers of glyC direct product formation. This is true since the break point for or against "wrong" isomer templating vis-à-vis yields is >25% $\geq n$+2-mer products for $glyC_2dC_5$ and >50% $\geq n$+1-mer products for $glyCdC_6$. It

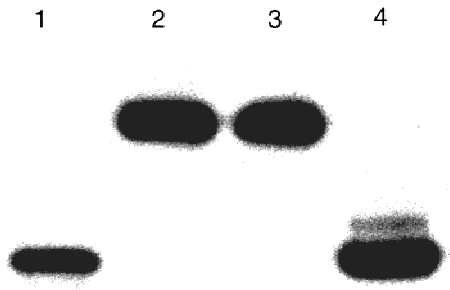

Fig. 5. Autoradiogram of 20% PAGE analysis of the oligomerization product derived from templates **5** after RNase T1 digestion. Lane 1, unreacted template **5;** lane 2, purified oligomerization product; lane 3, purified oligomerization product and buffer; lane 4, purified oligomerization product and buffer after incubation with RNase T1 for 12 h.

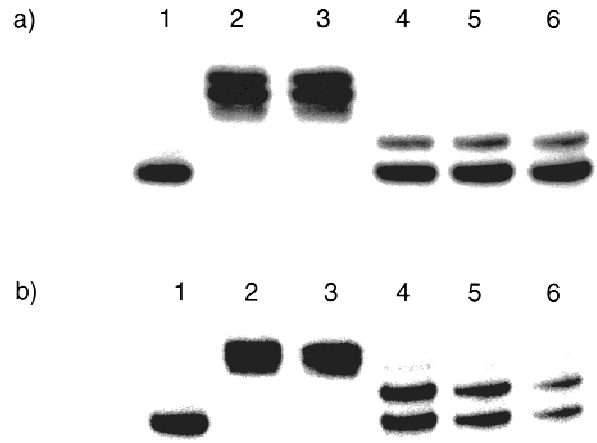

Fig. 6. Autoradiograms of 20% PAGE analyses of RNase T1 digests of the oligomerizations products from templates **6 (a)** and **7 (b).** Lane 1, unreacted template; lane 2, purified oligomerization product; lane 3, purified oligomerization product and buffer; lanes 4–6, purified oligomerization product and buffer after incubation with RNase T1 for 6, 12, and 24 h, respectively.

was not possible to resolve neighboring bands sufficiently to apply the test to the remaining two glyC templates.

Regiochemistry of Phosphodiester Bond Formation

The products obtained from the oligomerization of templates **5–7** were treated with the enzyme ribonuclease T1 to determine the regiochemical preference for phosphodiester bond formation between the primer and the *n*+1 adduct (Wu and Orgel 1992). RNase T1 specifically cleaves 3′,5′-phosphodiester bonds of any ribonucleotide located 3′ to a *ribo*G residue, producing a terminal 3′-monophosphate and a free 5′-OH group. As shown Fig. 5, the outcome of digesting the oligomerization product from a 10-day reaction on the natural dC_7 hairpin template, **1**, is nearly exclusively a single faster-moving band (lane 4) whose electrophoretic mobility is indistinguishable from that of the original hairpin template. This observation is in keeping with earlier findings of Orgel (Wu and Orgel 1992) and is consistent with the formation of a 3′,5′-phosphodiester linkage between the primer and the first 5′-GMP residue incorporated into the product during the oligomerization reaction. PAGE analyses of RNase T1 digests of products derived from templates $glyCdC_6$ and $glyC_2dC_5$ show two faster-moving bands (Figs. 6a and b, lanes 4–6). In both cases, the faster-moving band is electrophoretically indistinguishable from the original template and thus corresponds to a cleavage product whose parent incorporated a 3′,5′ linkage between the primer and the first 5′-GMP incorporated ($G_{(n)}$–3′-PO_2-5′–$G_{(n+1)}$), whereas the slower-moving band is consistent with the product derived from a parent bearing a 2′,5′ linkage at the same position ($G_{(n)}$–2′-PO_2-5′–$G_{(n+1)}$), as depicted in Fig. 7. Further examination of the digests suggests that template $glyCdC_6$ is capable of controlling the regiochemistry by a factor of >5:1 in favor of the 3′,5′ over the 2′,5′ linkage. In contrast, template $glyC_2dC_5$, which contains two consecutive glyC residues, does not exhibit any detectable degree of preference for the formation of 2′,5′- or 3′,5′-phosphodiester linkages for the first 5′-GMP residue incorporated. Apparently, two sequential acyclic residues confer sufficient template flexibility to result in a loss of control over the integrity of the product linkage, but a single such residue leaves a measure of control.

Thermodynamic Stability of Glyceryl Versus Deoxyribosyl Cytosine

Thermal denaturation profiles were obtained for the duplexes given in Table 1 to determine the effect of an internal atactic glyceryl cytosine residue on duplex stability. Representative denaturation profiles for several of the duplexes are shown in Fig. 8. The cooperative transition observed when oligonucleotides **11** and **13** are combined indicates the formation of a duplex incorporating the modified strand. Free energies of duplex formation were determined for the **11/13** duplex and other cases by nonlinear regression fitting of the denaturation profiles and are summarized in Table 1. Comparison of the table entries reveals that the atactic glyC–dG base-pair with a $\Delta\Delta G^\circ = -1.5$ kcal/mol is closest in stability to a standard dT · dA base-pair. Previously Benner has demonstrated that an isotactic glyT · dA base-pair is roughly equivalent energetically to a G · T mismatch (Schneider and Benner 1990). It would appear that both diastereomers of oligonucleotide **11** interact with oligonucleotide **13** given similar hyperchromicities and similar denaturation cooperativities (implied by similar curve shapes) for all three duplexes shown in Fig. 8. The stability of glyC–dG is consistent with the ability of glyC to participate in template-directed reactions.

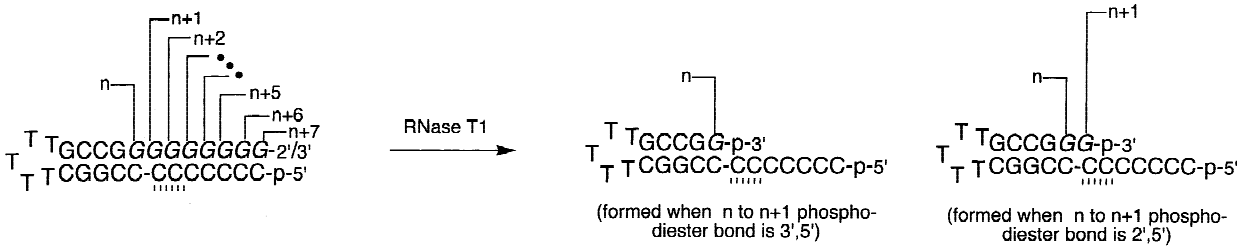

Fig. 7. Summary of the transformation consistent with the data in lanes 4–6 in Fig. 6.

Table 1. Summary of results obtained from thermal denaturation of the DNA duplexes indicated[a]

Entry	Oligonucleotide		T_m (°C)	$-\Delta G^0_{37}$ (kcal/mol)	$-\Delta\Delta G^0_{37}$ (kcal/mol)	$-\Delta\Delta G^{0\prime}_{37}$ (kcal/mol)
1	5′-dCTTTC**C**CTCCCT	**10**	57.0	13.5	0	1.5
	3′-dGAAAG**G**GAGGGA	**13**				
2	5′-dCTTTC**T**CTCCCT	**12**	54.1	12.8	−0.7	0.8
	3′-dGAAAG**A**GAGGGA	**14**				
3	5′-dCTTTC**C**CTCCCT	**11**	50.9	12.0	−1.5	0
	3′-dGAAAG**G**GAGGGA	**13**				
4	5′-dCTTTC**T**CTCCCT	**12**	45.4	10.5	−3.0	−1.5
	3′-dGAAAG**G**GAGGGA	**13**				

[a]**C** Corresponds to an atactic glyceryl cytosine residue. Errors in free energies are estimated to be less than 5%

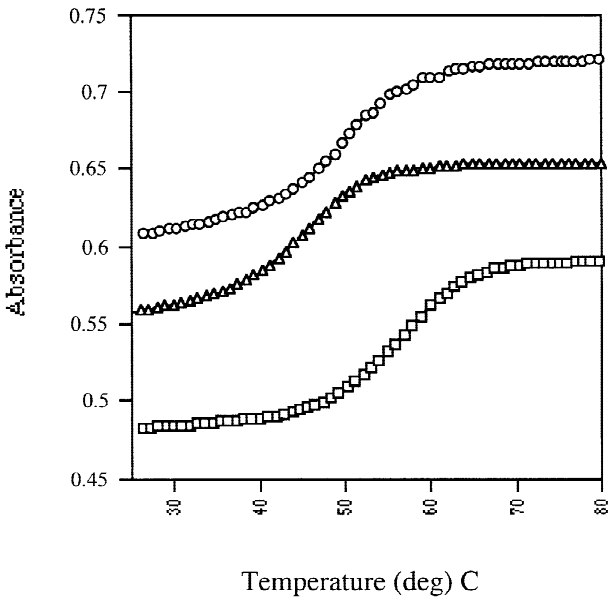

Fig. 8. UV absorbance (260 nm) versus temperature profile for **(a) 10** and **13** (□), **(b) 11** and **13** (○), and **(c) 12** and **13** (△).

Conclusions

In summary, templates containing *atactic* glyceryl cytosine residues direct the synthesis of oligoguanylate products with a diminished capacity compared to *isotactic* 2′-deoxyribocytidine templates. A more complete assessment of the effectiveness of atactic glyceryl nucleotide templates will have to await comparison with atactic rather than isotactic DNA or RNA. Based on the results reported here, it is clear that phosphodiester-linked acyclic nucleotides participate in template-directed synthetic reactions. This finding complements earlier studies of acyclic nucleic acids incorporating pyrophosphate linkages (Schwartz and Orgel 1985; Visscher and Schwartz 1988, 1990). It would thus seem conceivable that phosphodiester-linked acyclic nucleotides could have coexisted with other components of a (stereo)chemically heterogeneous primitive genetic system (Ertem and Ferris 1996).

Acknowledgments. This work was funded by grants from the NASA Astrobiology Institute and the NASA Exobiology Program.

References

Bolli M, Micura R, Eschenmoser A (1997) Pyranosyl-RNA: Chiroselective self-assembly of base sequences by ligative oligomerization of tetranucleotide-2′,3′-cyclophosphates. Chem Biol 4:309–320

Cairns-Smith AG (1982) Genetic takeover and the mineral origins of life. Cambridge University Press, Cambridge

Ertem G, Ferris JP (1996) Synthesis of RNA oligomers on heterogeneous templates. Nature 379:238–240

Frauendorf C, Jaschke A (1998) Catalysis of organic reactions by RNA. Angew Chem Int Ed Engl 37:1378–1381

Inoue T, Orgel LE (1981) Substituent control of the poly(C)-directed oligomerization of guanosine 5′-phosphoroimidazolide. J Am Chem Soc 103:7666–7667

Joyce GF (1987) Nonenzymatic template-directed synthesis of informational macromolecules. Cold Spring Harbor Symp Quant Biol LII:41–51

Joyce GF (1989) RNA evolution and the origins of life. Nature 338:217

Joyce GF (1996) Ribozymes—Building the RNA world. Curr Biol 6:965–967

Joyce GF, Schwartz AW, Miller SL, Orgel LE (1987) The case for an ancestral genetic system involving simple analogues of the nucleotides. Proc Natl Acad Sci USA 84:4398–4402

Joyce GF, Visser GM, van Boeckel CAA, van Boom JH, Orgel LE, van Westrenen J (1984a) Chiral selection in poly(C)-directed synthesis of oligo(G). Nature 310:602–604

Joyce GF, Inoue T, Orgel LE (1984b) Non-enzymatic template-directed synthesis on RNA random copolymers. J Mol Biol 176: 279–306

Kozlov IA, Politis PK, Pitsch S, Herdewijn P, Orgel LE (1999) A highly enantioselective hexitol nucleic acid template for nonenzymatic oligoguanylate synthesis. J Am Chem Soc 121:1108–1109

Larralde R, Robertson MP, Miller SL (1995) Rates of decomposition of ribose and other sugars—Implications for chemical evolution. Proc Natl Acad Sci USA 92:8158–8160

Longfellow CE, Kierzek R, Turner DH (1990) Thermodynamic and spectroscopic study of bulge loops in oligonucleotides. Biochemistry 29:278–285

Merle Y, Bonneil E, Merle L, Sagi J, Szemzo A (1995) Acyclic oligonucleotide analogues. Int J Biol Macromol 17:239–246

Ogilvie KK, Dixit DM, Radatus BR, Smith KO, Galloway KS (1983) Synthesis of 5-substituted-1-[[2-hydroxy-1-(hydroxylmethyl-)ethoxy]cytosines. Nucleosides Nucleotides 2:147–154

Orgel LE (1992) Molecular replication. Nature 358:203–209

Prakash TP, Roberts C, Switzer C (1997) Activity of 2′5′-linked RNA in the template-directed oligomerization of mononucleotides. Angew Chem Int Ed Engl 36:1522–1523

Schmidt JG, Nielsen PE, Orgel LE (1997) Enantiomeric cross-inhibition in the synthesis of oligonucleotides on a nonchiral template. J Am Chem Soc 119:1494–1495

Schneider KC, Benner SA (1990) Oligonucleotides containing flexible nucleoside analogues. J Am Chem Soc 112:453–455

Schwartz AW, Orgel LE (1985) Template-directed synthesis of novel nucleic acid-like structures. Science 228:585–587

Spach G (1984) Chiral versus chemical evolutions and the appearance of life. Origins Life 14:433–437

Tarasow TM, Tarasow SL, Eaton BE (1997) RNA-catalysed carbon-carbon bond formation. Nature 394:54–57

Unrau PJ, Bartel DP (1998) RNA-catalysed nucleotide synthesis. Nature 395:260–263

Visscher J, Schwartz AW (1988) Template-directed synthesis of acyclic oligonucleotide analogues. J Mol Evol 28:3–6.

Visscher J, Schwartz AW (1990) Template-catalyzed oligomerization with an atactic glycerol-based polynucleotide analog. J Mol Evol 31:163–166

Wu T, Orgel LE (1992) Nonenzymatic template-directed synthesis on hairpin oligonucleotides. J Am Chem Soc 114:322